Developmental Biology 446 (2019) 94–101

Contents lists available at ScienceDirect

Developmental Biology

journal homepage: www.elsevier.com/locate/developmentalbiology

FGFR1 regulates trophectoderm development and facilitates blastocyst implantation

Agata Kurowski[1], Andrei Molotkov[2], Philippe Soriano[*]

Department of Cell, Developmental, and Regenerative Biology, Icahn School of Medicine at Mount Sinai, New York, NY 10029, United States

ARTICLE INFO

Keywords:
FGF
Trophectoderm
TS cells

ABSTRACT

FGF signaling plays important roles in many aspects of mammalian development. *Fgfr1*$^{-/-}$ and *Fgfr1*$^{-/-}$ *Fgfr2*$^{-/-}$ mouse embryos on a 129S4 co-isogenic background fail to survive past the peri-implantation stage, whereas *Fgfr2*$^{-/-}$ embryos die at midgestation and show defects in limb and placental development. To investigate the basis for the *Fgfr1*$^{-/-}$ and *Fgfr1*$^{-/-}$ *Fgfr2*$^{-/-}$ peri-implantation lethality, we examined the role of FGFR1 and FGFR2 in trophectoderm (TE) development. *In vivo*, *Fgfr1*$^{-/-}$ TE cells failed to downregulate CDX2 in the mural compartment and exhibited abnormal apicobasal E-Cadherin polarity. *In vitro*, we were able to derive mutant trophoblast stem cells (TSCs) from *Fgfr1*$^{-/-}$ or *Fgfr2*$^{-/-}$ single mutant, but not from *Fgfr1*$^{-/-}$ *Fgfr2*$^{-/-}$ double mutant blastocysts. *Fgfr1*$^{-/-}$ TSCs however failed to efficiently upregulate TE differentiation markers upon differentiation. These results suggest that while the TE is specified in *Fgfr1*$^{-/-}$ mutants, its differentiation abilities are compromised leading to defects at implantation.

1. Introduction

By the time of implantation, the late mouse blastocyst consists of three segregated lineages, the epiblast (EPI), the primitive endoderm (PrE) and the trophectoderm (TE). Both the EPI and the PrE originate from the inner cell mass (ICM) and give rise to the fetus proper and components of the yolk sac, respectively. The outside cells form the TE epithelium and contribute to the placenta which supplies the embryo with nutrients.

Fibroblast Growth Factors (FGFs) signal through four FGF receptor tyrosine kinases (FGFR1-FGFR4) and engage a number of signaling pathways including ERK1/2, PLCγ and PI3K (reviewed in Brewer et al. (2016)). FGF signaling plays an important role in preimplantation development. This was initially demonstrated in *Fgf4*$^{-/-}$ mice which die at the peri-implantation stage (Feldman et al., 1995; Goldin and Papaioannou, 2003; Kang et al., 2013). Further analyses revealed that the FGF/MEK/ERK1/2 signaling pathway plays an essential role in the specification of the PrE (Brewer et al., 2015; Chazaud et al., 2006; Kang et al., 2017, 2013; Molotkov et al., 2017; Molotkov and Soriano, 2018; Nichols et al., 2009; Yamanaka et al., 2010).

Previous publications have shown that on a mixed genetic background, a proportion of *Fgfr1*$^{-/-}$ embryos are lost prior to or at gastrulation (Ciruna and Rossant, 2001; Deng et al., 1994; Kang et al., 2017; Yamaguchi et al., 1994), with cells failing to complete the epithelial to mesenchymal (EMT) transition required for mesoderm formation (Ciruna and Rossant, 2001). On a co-isogenic 129S4 genetic background however, *Fgfr1*$^{-/-}$ embryos show increased number of epiblast cells at the expense of PrE cells and fail to progress beyond implantation (Brewer et al., 2015). It was recently shown that loss of both *Fgfr1* and *Fgfr2* leads to the complete absence of PrE cells, with *Fgfr1* playing the predominant role (Kang et al., 2017; Molotkov et al., 2017). *Fgfr1*$^{-/-}$ *Fgfr2*$^{-/-}$ double mutants also fail to progress past implantation (Kang et al., 2017; Molotkov et al., 2017). However, an intrinsic deficiency that would affect only the PrE is unlikely to explain peri-implantation lethality, and we therefore sought to examine TE development.

FGF signaling plays an important role in placental development and is required for the derivation of trophoblast stem cells (TSCs) from the TE (Tanaka et al., 1998). Removal of FGF4 from culture medium leads to TSC differentiation into giant cells (Tanaka et al., 1998). An important mediator of FGF signaling, ERK2, has been shown to regulate TE development and the development of the placenta (Hatano et al., 2003; Saba-El-Leil et al., 2003). Furthermore, it has been shown that the binding and phosphorylation of the adaptor protein FRS2, which links FGFR1 to ERK1/2 signaling, is essential for TSC self-renewal and proliferation (Ong et al., 2000).

* Corresponding author.
E-mail address: philippe.soriano@mssm.edu (P. Soriano).
[1] Present address: Department of Pharmacological Sciences, Icahn School of Medicine at Mount Sinai, New York, NY 10029, USA.
[2] Present address: Department of Radiology, Columbia University School of Medicine, New York, NY 10032, USA.

https://doi.org/10.1016/j.ydbio.2018.12.008
Received 19 November 2018; Received in revised form 10 December 2018; Accepted 11 December 2018
Available online 12 December 2018

Here we show that *in vivo,* FGFR1 and FGFR2 are strongly expressed in the TE of newly implanted blastocysts at Embryonic day (E) 4.5 and in the extraembryonic ectoderm at E5.5. We find that E4.5 *Fgfr1*$^{-/-}$ embryos show altered TE cell morphology and E-Cadherin expression, and fail to downregulate Cdx2 in the mural TE where implantation is initiated. Interestingly, *Fgfr1*$^{-/-}$ TSCs could be derived and cultured indefinitely, but show diminished expression of TE lineage markers upon removal of FGF from culture medium. This suggests that *in vitro Fgfr1* is dispensable for TSC proliferation and maintenance, but may be required for further differentiation along specific TE lineages. *Fgfr2*$^{-/-}$ TSCs could be isolated and showed no defects in differentiation. However, we were unable to recover *Fgfr1*$^{-/-}$ *Fgfr2*$^{-/-}$ double null TSCs. These results indicate an important role for FGF signaling through FGFR1/2 in TE development, implantation and in TSC establishment and differentiation.

2. Materials and methods

2.1. Mice

Fgfr1$^{lox/lox}$ mice (Hoch and Soriano, 2006), *Fgfr2*$^{lox/lox}$ mice (Molotkov et al., 2017), *Fgfr1*$^{T2A\text{-}H2B\text{-}GFP}$ further referred to as *Fgfr1*^{GFP} (Molotkov et al., 2017), *Fgfr2*$^{T2A\text{-}H2B\text{-}mCherry}$ mice further referred to as *Fgfr2*^{mCherry} (Molotkov et al., 2017) were maintained on a 129S4/SvJaeSor (MGI:3044540) co-isogenic background, further referred to as 129. *Fgfr1*$^{-}$ and *Fgfr2*$^{-}$ alleles were generated from the floxed alleles by crossing with epiblast specific *Meox2*^{Cre} mice (Tallquist and Soriano, 2000), also on the 129 background, and subsequently crossing out the *Cre* driver. All animal experimentation was conducted according to protocols approved by the Institutional Animal Care and Use Committee of Icahn School of Medicine at Mount Sinai.

2.2. Cell culture and manipulation

AK7.1 mouse embryonic stem cells (ESCs) were cultured in 2i/LIF as described (Kunath et al., 2007; Mulas et al., 2017). Wild-type and *Fgfr1*$^{-/-}$ *Fgfr2*$^{-/-}$ ESCs were transfected with a linearized pPyCAG-Cdx2^{ERT2}-IP plasmid (Niwa et al., 2005) using Lipofectamine 2000 and cells were selected with 2 μg/ml puromycin. Stably transfected and resistant clones were picked and expanded. The resulting ESCs lines were cultured for two weeks in TSC medium (Ohinata and Tsukiyama, 2014) with 1 μg/ml 4-hydroxytamoxifen (4-OHT) to induce *Cdx2* expression and obtain TSC colonies on fibronectin.

TSCs from E4.5 blastocysts were derived and cultured in N2B27 complemented with 5 nM Y27632, 10 nM XAV939, 20 ng/ml Activin A and 12.5 ng/ml FGF2 as described (Ohinata and Tsukiyama, 2014). *Fgfr1*$^{floxed/floxed}$*Fgfr2*$^{floxed/floxed}$ and *Fgfr1*$^{floxed/+}$*Fgfr2*$^{floxed/+}$ TSCs were transfected with Cre-IRES-Blasticidin or linearized Cre^{ERT2}-IRES-Blasticidin plasmids (Betschinger et al., 2013) using Lipofectamine 2000. The resulting TSCs colonies were cultured for 24 h in TSC medium with 1 μg/ml 4-hydroxytamoxifen (4-OHT) to induce Cre recombination and selected 48 h with 1 μg/ml blasticidin. pPyCAG-Cdx2^{ERT2}-IP, Cre-IRES-Blasticidin and Cre^{ERT2}-IRES-Blasticidin were kindly provided by Austin Smith and Ken Jones.

2.3. Embryo dissection and culture

Homozygous *Fgfr1*^{GFP}*Fgfr2*^{mCherry}, or *Fgfr1*$^{+/-}$ male and female mice were naturally mated and checked every morning for the appearance of a vaginal plug on E0.5. E3.5 embryos were flushed from the uterus and cultured in DMEM for 48 h. E4.5 and E5.5 embryos were dissected from the uterus and processed for immunostaining.

2.4. RT-qPCR

mRNA from TSCs was isolated using QIAGEN RNA-easy kit (74106, Qiagen), cDNA was prepared using Superscript II first strand system (18064014, Invitrogen). qPCR was run on an iQ5 multicolor real-time PCR detection system (BioRad) using Perfecta Sybr Green master mix (101414-264, VWR). All primer sequences were derived from qPrimerDepot (Cui et al., 2007) and exon-exon spanning pairs were chosen as shown in Supplementary Table 1. Graphs were created using Excel.

2.5. Immunofluorescence staining

Immunostaining was performed essentially as described (Nichols et al., 2009). Embryos or TSCs were fixed 15 min in 4% PFA, permeabilized for 30 min in 0.5% Triton X100 (T9284, Sigma) and 3 mg/ml PVP in PBS, blocked in 0.1% BSA with 2% donkey serum in 0.25% Triton X100 in PBS/PVP for a minimum of 30 min and incubated overnight with primary antibodies used at 1/200 dilution. Primary antibodies used: NANOG (Cosmo Bio Co., Ltd, RCAB0002P-F), CDX2 (MU392A-UC, BioGenex), GATA6 (AF1700, R & D Systems), E-Cadherin (R & D Systems, AF1700), GFP (Invitrogen A6455), mCHERRY (Abcam ab167453), OCT3/4 (Santa Cruz, sc-5279). On the next day, embryos were washed in PBST and incubated for 1 h with secondary Alexa Fluor (Invitrogen) conjugated antibodies diluted 1/500 in 1% donkey serum in PBST. Blastocysts and TSCs were counter-stained with DAPI and mounted in Vectashield. Confocal images were taken using a Leica TCS SP5 confocal microscope. Optical section images were taken on a Zeiss Axio-Observer Z1 with an Apotome 2 attachment, using a Hamamatsu Orca Flash 4.0 LT camera and ZenPro 2015 software. LAS AF Lite was used to visualize confocal images and to create the intensity heat maps using the pre-defined LUT spectrum visualization settings. PAST 3.19 Paleontological Statistics software (Hammer et al., 2001) was used to create the box plot graphs.

3. Results

3.1. FGFR1 and FGFR2 are highly expressed in TE lineages of peri- and post-implantation embryos and in TSCs in vitro

To assess the expression of *FGFR1* and *FGFR2* in the peri-implantation embryo and in TSCs, we used our previously described *Fgfr1*^{GFP} and *Fgfr2*^{mCHERRY} fluorescent knock-in reporter mouse lines, in which we had shown that both receptors are co-expressed in the TE at E3.5 (Molotkov et al., 2017). To assess *FGFR1/2* expression at later stages, we dissected E4.5 and E5.5 embryos from decidua and show that *Fgfr1*^{GFP} is expressed more strongly in the TE and extraembryonic ectoderm than in the OCT4^{+} epiblast (EPI) cells (Fig. 1A, B). *Fgfr2*^{mCHERRY} is strongly expressed in the TE at E4.5 and in the extraembryonic ectoderm and visceral endoderm in E5.5 embryos. It is faintly detectable in Oct4^{+} EPI cells at E4.5, and is absent in the E5.5 EPI (Fig. 1A, B). Both reporters are expressed in CDX2^{+} TSCs derived from *Fgfr1*$^{GFP/GFP}$*Fgfr2*$^{mCHERRY/mCHERRY}$ blastocysts (Fig. 1C). Taken together, these results show that FGFR1 and FGFR2 are co-expressed in TE and TE derived cells, as well as in TSCs *in vitro*.

3.2. Fgfr1$^{-/-}$ blastocysts fail to maintain TE polarity

Next, we examined *Fgfr1*$^{-/-}$ blastocysts at implantation (E4.5) just prior to *Fgfr1*$^{-/-}$ lethality on the 129 background (Brewer et al., 2015). We investigated TE development by following the expression of CDX2 in E4.5 blastocysts. At this stage the mural TE differentiates into giant cells to ensure implantation of the embryo. CDX2 was downregulated in the mural TE of control blastocysts (Fig. 2A). Remarkably, CDX2 expression was maintained at high levels in *Fgfr1*$^{-/-}$ blastocysts throughout the TE (Fig. 2B), suggesting a differentiation defect. A

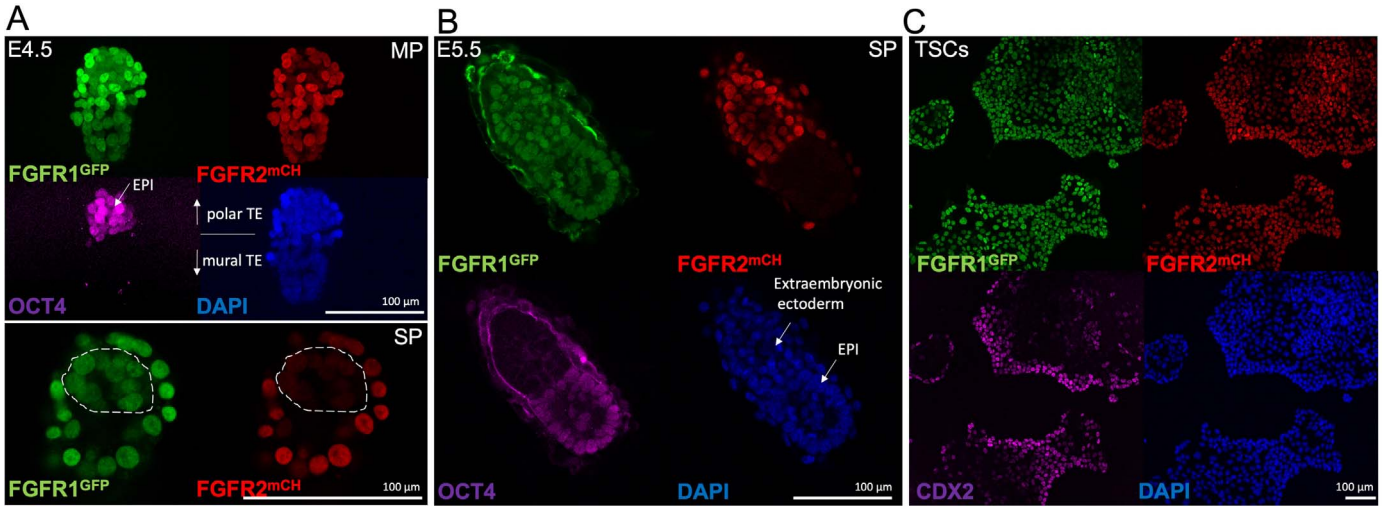

Fig. 1. FGFR1 and FGFR2 are expressed in the TE and the extraembryonic ectoderm. A, Maximal projection (MP) of confocal immunofluorescence images of FGFR reporter embryos showing strong $FGFR1^{GFP}$ and $FGFR2^{mCHERRY}$ expression in the TE of E4.5 blastocysts. OCT4 expression marks the EPI. The single plane (SP) image through the EPI clearly detects $FGFR1^{GFP}$ expression in the ICM, whereas $FGFR2^{mCHERRY}$ is weakly expressed. The dashed line was drawn around cells which expressed OCT4. B, at E5.5 $FGFR1^{GFP}$ is expressed throughout embryonic- and extra-embryonic tissues. $FGFR2^{mCHERRY}$ is restricted to the extraembryonic ectoderm. OCT4 marks the EPI. C, both receptors are expressed in CDX2 positive TSCs. DAPI shows nuclei.

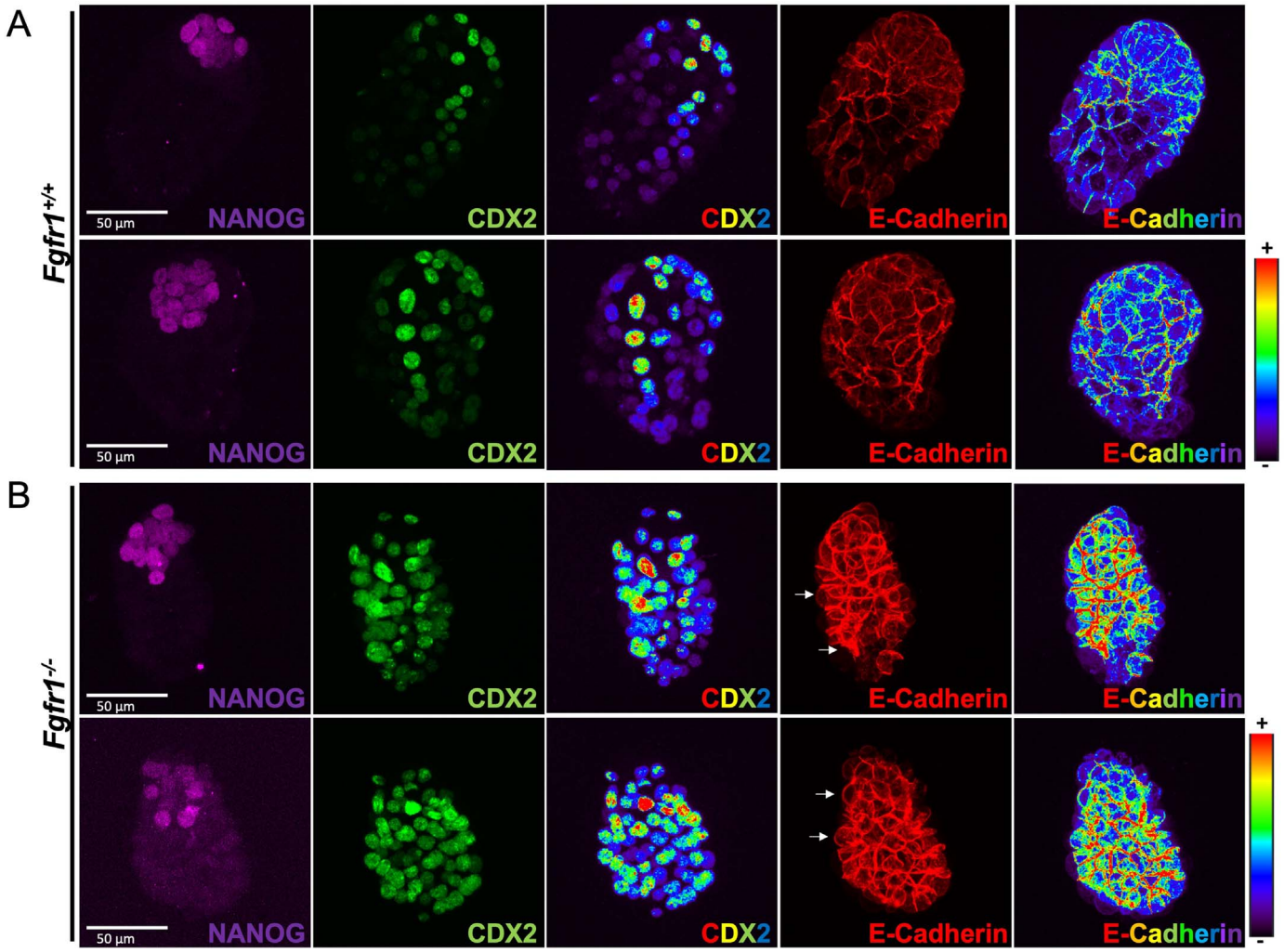

Fig. 2. E4.5 *FGFR1*$^{-/-}$ TE is specified but the expression of CDX2 and E-Cadherin is abnormal. A and B, maximal projection confocal immunofluorescence images of wild type and *Fgfr1*$^{-/-}$ E4.5 blastocysts showing NANOG, CDX2 and E-Cadherin expression. A, wild type E4.5 blastocysts show downregulated CDX2 expression in the mural TE and basolateral E-Cadherin expression in TE cells. NANOG marks the EPI cells. Heat maps show the intensity of CDX2 and E-Cadherin expression. B, *Fgfr1*$^{-/-}$ blastocysts maintain high CDX2 expression throughout the TE and show strong basolateral and abnormal apical E-Cadherin expression (arrows).

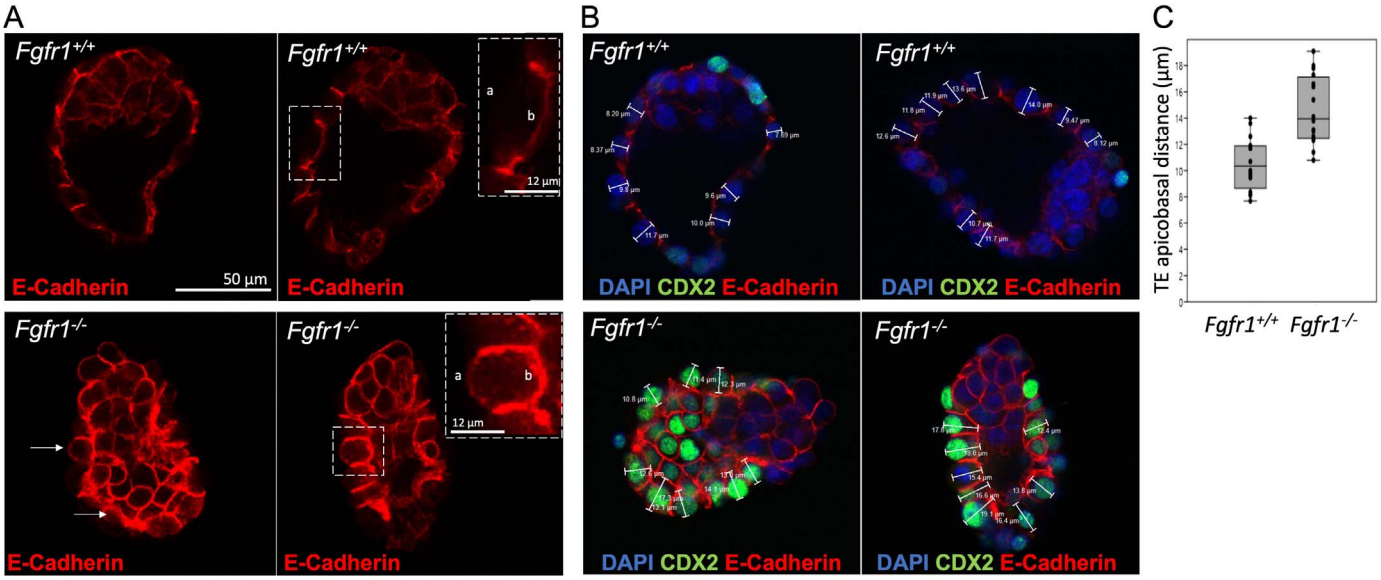

Fig. 3. *Fgfr1*$^{-/-}$ blastocysts at E4.5 show abnormal TE cell polarity and an increased apicobasal distance. A, Single plane confocal immunofluorescence image of wild type and *Fgfr1*$^{-/-}$ E4.5 blastocysts showing basolateral E-Cadherin expression in TE cells and basolateral and apical expression in *Fgfr1*$^{-/-}$. Insets show enlarged single TE cells and depict the apical (a) and basal (b) cell membranes. B and C, confocal plane section images showing that the apicobasal distance of TE cells of *Fgfr1*$^{-/-}$ embryos is increased in comparison to TE cells of control embryos. C, quantification of TE cell apicobasal distance of two *Fgfr1*$^{+/+}$ and two *Fgfr1*$^{-/-}$ embryos. Cells measured in A and B are quantified in C.

characteristic of the TE is its tight junctions between cells which maintain the blastocoel cavity (Fleming and Johnson, 1988). Another important cell interaction between adjacent cells in the TE are the adherens junctions (Fleming et al., 1991). We therefore analyzed expression of E-Cadherin, which localizes to the basolateral adherens junctions. While E-Cadherin expression was restricted to the basolateral membranes in wild type TE cells (Fig. 2A, Fig. 3A), *Fgfr1*$^{-/-}$ TE cells exhibited very strong basal expression as well as additional apical E-Cadherin localization (Fig. 2B, Fig. 3A). Heatmaps in Fig. 2 show the intensity of CDX2 and E-Cadherin expression throughout the blastocysts (blue low, red high), both proteins are visibly more highly expressed in *Fgfr1*$^{-/-}$ TE cells. These phenotypes were 100% penetrant in *Fgfr1*$^{-/-}$ blastocysts (n = 7) and strikingly similar to that observed in *Cdx2*$^{-/-}$ blastocysts which also fail to generate a functional TE and show peri-implantation lethality (Strumpf et al., 2005). Additionally, we observed an increase in the apicobasal distance of TE cells of *Fgfr1*$^{-/-}$ embryos, relative to control (Fig. 3B, C), which may reflect a loss of cell tension within the TE. In turn, the abnormal apposition of TE cells may lead to a leaky epithelial lining surrounding the blastocoel cavity, explaining why none of the *Fgfr1*$^{-/-}$ blastocysts showed a fully expanded cavity (Fig. 3). Although all *Fgfr1*$^{-/-}$ embryos hatched out of their zona pellucida, the trophectoderm defect may subsequently interfere with implantation (White et al., 2018).

Interestingly, E4.5 *Fgfr1*$^{-/-}$ embryos could only be recovered in Mendelian proportions (6/19) by flushing the uterus. Attempts to dissect embryos from implantation sites at E4.5 only yielded two *Fgfr1*$^{-/-}$ embryos among 47 blastocysts, with no increase in the proportion of empty decidua. Taken together, these results suggest that *Fgfr1*$^{-/-}$ TE cells show altered polarity and fail to differentiate, hindering embryo implantation.

3.3. *Fgfr1*$^{-/-}$ TSCs exhibit a defective differentiation potential

To further investigate the requirement of *Fgfr1* in TE development, we sought to derive *Fgfr1*$^{-/-}$ TSCs. Blastocysts were obtained from heterozygous *Fgfr1*$^{+/-}$ mouse intercrosses and TSCs were derived in chemically defined culture medium (Ohinata and Tsukiyama, 2014). We successfully derived TSCs from eighty-three E3.5 blastocyst outgrowths obtained from super ovulated females, twenty of these were genotyped by PCR as *Fgfr1*$^{-/-}$. *Fgfr1*$^{-/-}$ TSCs showed no morphological differences compared to wild type or heterozygous TSCs (Fig. 4A) and could be propagated for over 20 passages. Using immunofluorescence, we found that wild type and mutant TSCs showed robust CDX2 expression and no expression of the pluripotency marker NANOG or the PrE marker GATA6 (Fig. 4B). *Fgfr1* mRNA was absent in *Fgfr1*$^{-/-}$ TSCs (Fig. 4C). To test whether *Fgfr2* is upregulated in *Fgfr1*$^{-/-}$ TSCs we performed further RT-qPCRs. In *Fgfr1*$^{-/-}$ *and Fgfr1*$^{+/+}$ TSCs the levels were similar, indicating no compensation by *Fgfr2* in mutant cells (Fig. 4C). In contrast to the results obtained *in vivo*, E-Cadherin showed no differences in protein levels and localization, or mRNA expression (Fig. 4D). To further characterize the TSC lines, we analyzed the expression of TSC and TE differentiation markers. The expression of TSC markers showed no significant alterations in *Fgfr1*$^{-/-}$ TSCs compared to control cell lines (Fig. 4E). However, the differentiation markers *Dlx3* (labyrinthine layer), *Hand1* (giant cells) and *Mash2* (spongiotrophoblast) showed significantly lower expression in *Fgfr1*$^{-/-}$ TSCs (Fig. 4F). This might indicate an altered differentiation potential of *Fgfr1*$^{-/-}$ TSCs, consistent with our *in vivo* observations. To further assess the differentiation potential of *Fgfr1*$^{-/-}$ TSCs, we removed FGF4 from the culture medium, which forces wild type TSCs to spontaneously differentiate into all three TE lineages (Ohinata and Tsukiyama, 2014). Differentiated *Fgfr1*$^{-/-}$ or wild type cells showed no morphological differences (Fig. 5A). The expression of *Cdx2*, *Eomes* and *Elf5* was downregulated 24 h and 48 h following FGF removal in both wild type and *Fgfr1*$^{-/-}$ lines (Fig. 5B) and showed no significant differences. However, *Fgfr1*$^{-/-}$ TSCs failed to upregulate the expression of TE-derived lineage markers *Dlx3*, *Mash2* and *Hand1* to the same extent as wild type TSCs (Fig. 5C), further supporting an inherent defect in differentiation.

3.4. *Fgfr1*$^{-/-}$ *Fgfr2*$^{-/-}$ *blastocyst show reduced numbers of TE and double null TSCs are not viable*

We next attempted to derive *Fgfr2*$^{-/-}$ TSC lines from *Fgfr2*$^{+/-}$ intercrosses. *Fgfr2*$^{-/-}$ embryos die at E10.5 and show defects in the labyrinthine layer of the placenta, a derivative of the TE (Molotkov et al., 2017; Xu et al., 1998; Yu et al., 2003). We were able to derive *Fgfr2*$^{-/-}$ TSCs, in agreement with the late *Fgfr2*$^{-/-}$ phenotype. From four blastocyst outgrowths, two were *Fgfr2*$^{-/-}$, one *Fgfr2*$^{+/-}$ and one *Fgfr2*$^{+/+}$ (Fig. S1A). The morphology of *Fgfr2*$^{-/-}$ TSCs was comparable to wild

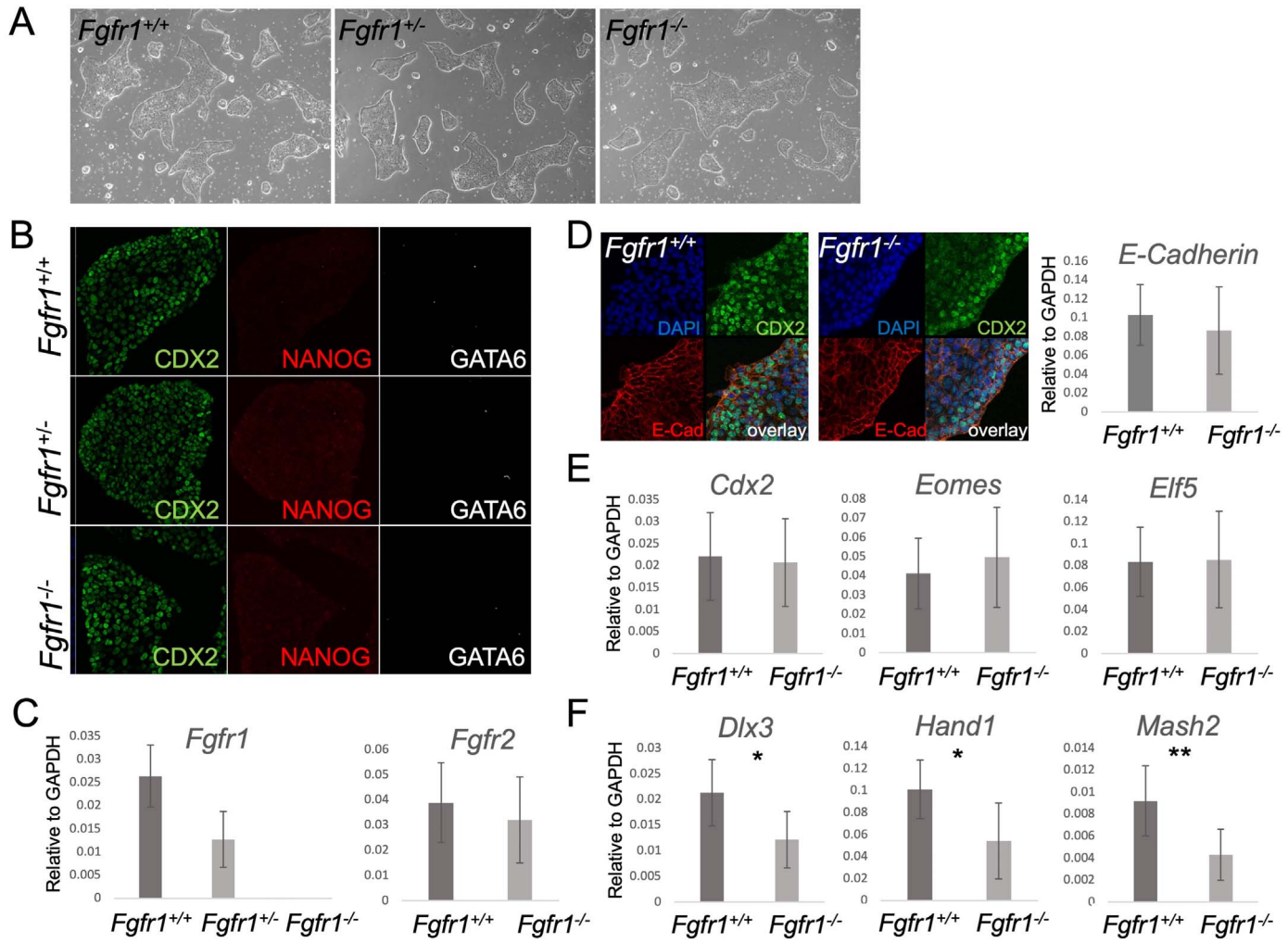

Fig. 4. *Fgfr1*$^{-/-}$ TSCs can be derived and maintained in culture. A, brightfield images showing similar morphology of control and *Fgfr1*$^{-/-}$ TSCs. B, confocal immunofluorescence images, showing the expression of the TSC marker CDX2 and absence of PrE or EPI blastocyst markers (GATA6 and NANOG) in derived TSC lines. C, RT-qPCR confirming the loss of *Fgfr1* mRNA in *Fgfr1*$^{-/-}$ TSCs and showing unchanged *Fgfr2* levels. D, Immunofluorescence and RT-qPCR, showing unchanged E-Cadherin protein expression and mRNA levels in control and mutant TSCs. E, RT-qPCR for TSCs markers showing no significant changes in *Fgfr1*$^{-/-}$ compared to wild type TSCs. F, RT-qPCR showing significantly lower expression of TE lineage markers in differentiated *Fgfr1*$^{-/-}$ compared to wild type TSCs. C-F: graphs represent three individually derived wild type TSC lines and three individually derived *Fgfr1*$^{-/-}$ TSC lines. * $P < 0.05$; ** $P < 0.01$; *** $P < 0.001$.

type lines (Fig. S1B) and the cells showed normal levels of *Cdx2* mRNA (Fig. S1C). After 72 h and 96 h without FGF, *Fgfr2*$^{-/-}$ TSCs down-regulated TSC markers and upregulated TE lineage markers (Fig. S1D, E). These results show that TSCs can be established and differentiated in the absence of FGFR2.

Next, we analyzed *Fgfr1*$^{-/-}$ *Fgfr2*$^{-/-}$ embryos, which fail to develop past E4.5 (Kang et al., 2017; Molotkov et al., 2017). We had previously demonstrated that double mutant embryos are smaller than wild-type embryos, but that they have a similar number of ICM cells (Molotkov et al., 2017), suggesting that the size reduction is due to a deficiency in TE development. We cultured E3.5 embryos for 48 h (Fig. 6A, B) and counted the number of CDX2^{+} TE cells. The number of CDX2^{+} TE cells in *Fgfr1*$^{-/-}$ *Fgfr2*$^{-/-}$ blastocyst was nearly half the level of *Fgfr1*$^{+/+}$ *Fgfr2*$^{+/+}$ blastocysts (Fig. 6B). This demonstrate that TE development is compromised in *Fgfr1*$^{-/-}$ *Fgfr2*$^{-/-}$ mutants.

We next attempted to derive *Fgfr1*$^{-/-}$ *Fgfr2*$^{-/-}$ double mutant TSCs. Because of the low frequency (1/16) of double mutants from double heterozygous intercrosses, we approached this by trying to convert *Fgfr1*$^{-/-}$ *Fgfr2*$^{-/-}$ ESCs (Molotkov et al., 2017) into TSCs by CDX2 overexpression (Niwa et al., 2005). Control and *Fgfr1*$^{-/-}$ *Fgfr2*$^{-/-}$ ESCs were stably transfected with a 4-OHT inducible *Cdx2* vector (Niwa et al., 2005). CDX2 expression was successfully induced with 4-OHT in TSC medium and ESCs downregulated the pluripotency marker NANOG; as expected, the PrE marker GATA6 was not detectable before or after 4-OHT treatment (Fig. 6C). Seven TSC clones were obtained from eight wild type transfected ESC lines (Fig. 6D). In contrast, none of six transfected *Fgfr1*$^{-/-}$ *Fgfr2*$^{-/-}$ lines gave rise to TSC colonies (Fig. 6D).

To independently validate these results, we derived *Fgfr1*$^{flox/+}$*Fgfr2*$^{flox/+}$ and *Fgfr1*$^{flox/flox}$*Fgfr2*$^{flox/flox}$ TSCs from blastocysts. We transiently transfected both lines with a Cre-IRES-Blasticidin vector. We assessed CRE activity by PCR of the recombined *Fgfr2* locus. After a short blasticidin selection, we observed CRE recombination in four out of eleven double heterozygous lines. In contrast none out of thirty-one double homozygous lines showed recombination (data not shown). In parallel, we stably transfected both cell lines with a Cre^{ERT2}-IRES-Blasticidin vector. Blasticidin-resistant clones were expanded and *Cre* presence was confirmed by PCR. Two out of three heterozygous control lines showed CRE recombination after 4-OHT administration (Fig. 6E). *Fgfr1*$^{flox/flox}$ *Fgfr2*$^{flox/flox}$ cultures, however, exhibited high cell death as evidenced by increased numbers of floating cells (Fig. 6F). Of the ten *Fgfr1*$^{flox/flox}$*Fgfr2*$^{flox/flox}$ TSC clones that nevertheless could be picked, none showed evidence for CRE induced DNA recombination (Fig. 6E). Taken together, these results show that even though TSCs can tolerate the absence of one or the other FGFR, the loss of both FGFR1 and FGFR2 does not allow TSCs to be maintained and propagated.

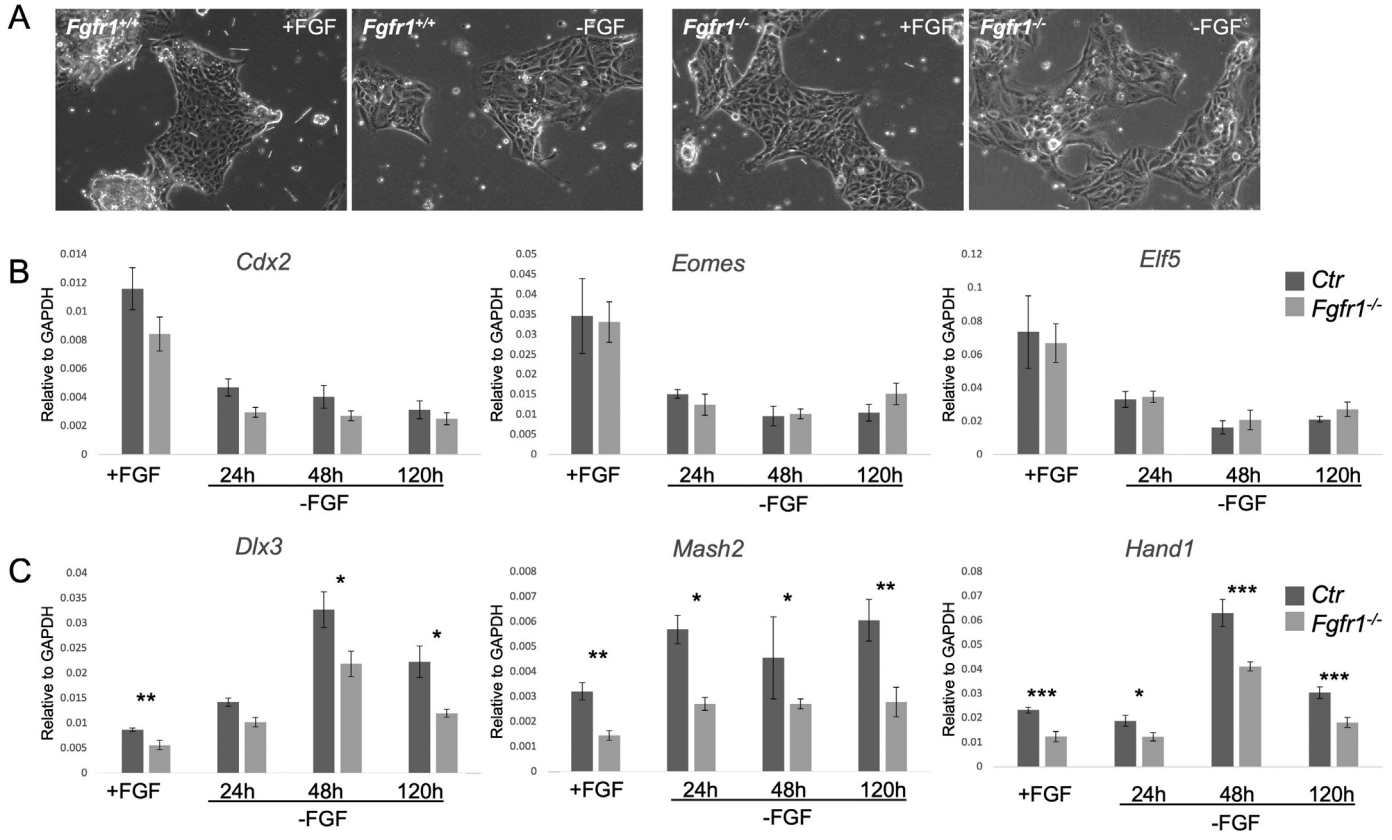

Fig. 5. *Fgfr1*$^{-/-}$ TSCs differentiation is impaired. A, brightfield images, showing that wild type and *Fgfr1*$^{-/-}$ TSCs become larger and less dense upon FGF removal for two days. No morphological differences can be detected between wild type and mutant cells. B, mRNA levels of TSC markers are downregulated equally in wild type and *Fgfr1*$^{-/-}$ TSCs. C, TE lineage markers are not upregulated to the same extent in *Fgfr1*$^{-/-}$ TSCs compared to wild type. B and C: Graphs represent technical triplicates of the same TSC line. * $P < 0.05$; ** $P < 0.01$; *** $P < 0.001$.

4. Discussion

FGFR1 is known to play a critical role at gastrulation (Deng et al., 1994; Yamaguchi et al., 1994) but a number of *Fgfr1*$^{-/-}$ mutants fail to progress past implantation, an effect most marked on the co-isogenic 129 genetic background (Brewer et al., 2015; Kang et al., 2017; Molotkov et al., 2017). Loss of both *Fgfr1* and *Fgfr2* leads to the complete absence of PrE development, with *Fgfr1* playing the predominant role, which may contribute to early postimplantation failure. FGFR1 also plays a role in regulating various stages of EPI differentiation (Kang et al., 2017; Molotkov et al., 2017). However, it is unlikely that PrE or EPI deficiency alone could explain the failure for mutant embryos to progress through the peri-implantation stage (Jedrusik et al., 2015). Indeed, chimeric embryos derived from *Fgfr1*$^{-/-}$ ES cells and wild type tetraploid embryos successfully implant, but later exhibit defects in mesoderm formation (Ciruna et al., 1997). This further supports the notion that FGF signaling is important for extraembryonic lineage development. In this work, we have identified a defect in TE development in *Fgfr1*$^{-/-}$ and *Fgfr1*$^{-/-}$ *Fgfr2*$^{-/-}$ embryos, which might lead to failure at implantation.

During the compaction stage in preimplantation development, individual blastomeres undergo apicobasal polarization. Polarized cell divisions persist such that outside cells retain an apical side and remain at the surface while apolar cells adopt an internal position (Johnson and Ziomek, 1981; further reviewed in Stephenson et al., 2012; White et al., 2018). Cell polarization is thus critical for normal development, and *Cdh1*$^{-/-}$ mutants lacking both maternal and zygotic E-Cadherin expression exhibit abnormal morphology of TE cells (Stephenson et al., 2010). We observed that *Fgfr1*$^{-/-}$ blastocysts show altered E-Cadherin polarized expression in TE cells, with strong basal expression, very similar to the phenotype observed in *Cdx2*$^{-/-}$ mutants (Strumpf et al., 2005). In intestinal epithelial cells, CDX2 enhances trafficking of E-Cadherin to the cell membrane (Funakoshi et al., 2010), whereas conditional loss of *Cdx2* leads to a strikingly similar alteration in E-Cadherin polarization as we have observed (Gao and Kaestner, 2010). Taken together, these observations suggest that CDX2 levels have to be maintained at specific levels to ensure proper apicobasal polarity. A connection between *Fgfr1* and *Cdh1* expression has been made previously, as *Fgfr1*$^{-/-}$ embryos on a mixed genetic background fail to downregulate E-Cadherin and complete EMT at the primitive streak (Ciruna and Rossant, 2001). Moreover, it has been shown recently that FGF signaling in *Drosophila* controls EMT by regulating apicobasal polarity, as *Heartless* (*Fgfr*) mutants exhibit reduced numbers of adherens junctions and defects in mesodermal cell polarity (Sun and Stathopoulos, 2018). These observations raise the additional possibility that elevated *Cdh1* expression in *Fgfr1*$^{-/-}$ TE cells may interfere with subsequent EMT associated with later stages of TE cell differentiation.

Fgfr1$^{-/-}$ mutants maintained CDX2 expression in the mural TE, similar to *Cdh1*$^{-/-}$ mutants. CDX2 is highly expressed in the mural TE at E3.5, and is then downregulated by the time of implantation. The significance of CDX2 expression in the mural TE cells at E3.5 remains unexplored, however, it may be required to inhibit OCT4 and NANOG expression as it does at the morula stage (Blij et al., 2012; Jedrusik et al., 2015; Strumpf et al., 2005). Moreover, CDX2 has been shown to directly interact with OCT4 to suppress its transcriptional activity in TE cells (Niwa et al., 2005). Last, as a pro-epithelial factor, CDX2 may be regulating TE fate both through *Nanog* and *Oct4* inhibition as well as promoting *Eomes* and *Elf5* expression. It may also allow junction formation that supports blastocoel establishment and maintenance. At a later stage CDX2 would need to be downregulated to reduce epithelial protein expression and to allow for protrusive activity and partial EMT required for implantation (Sutherland, 2003). It is therefore possible

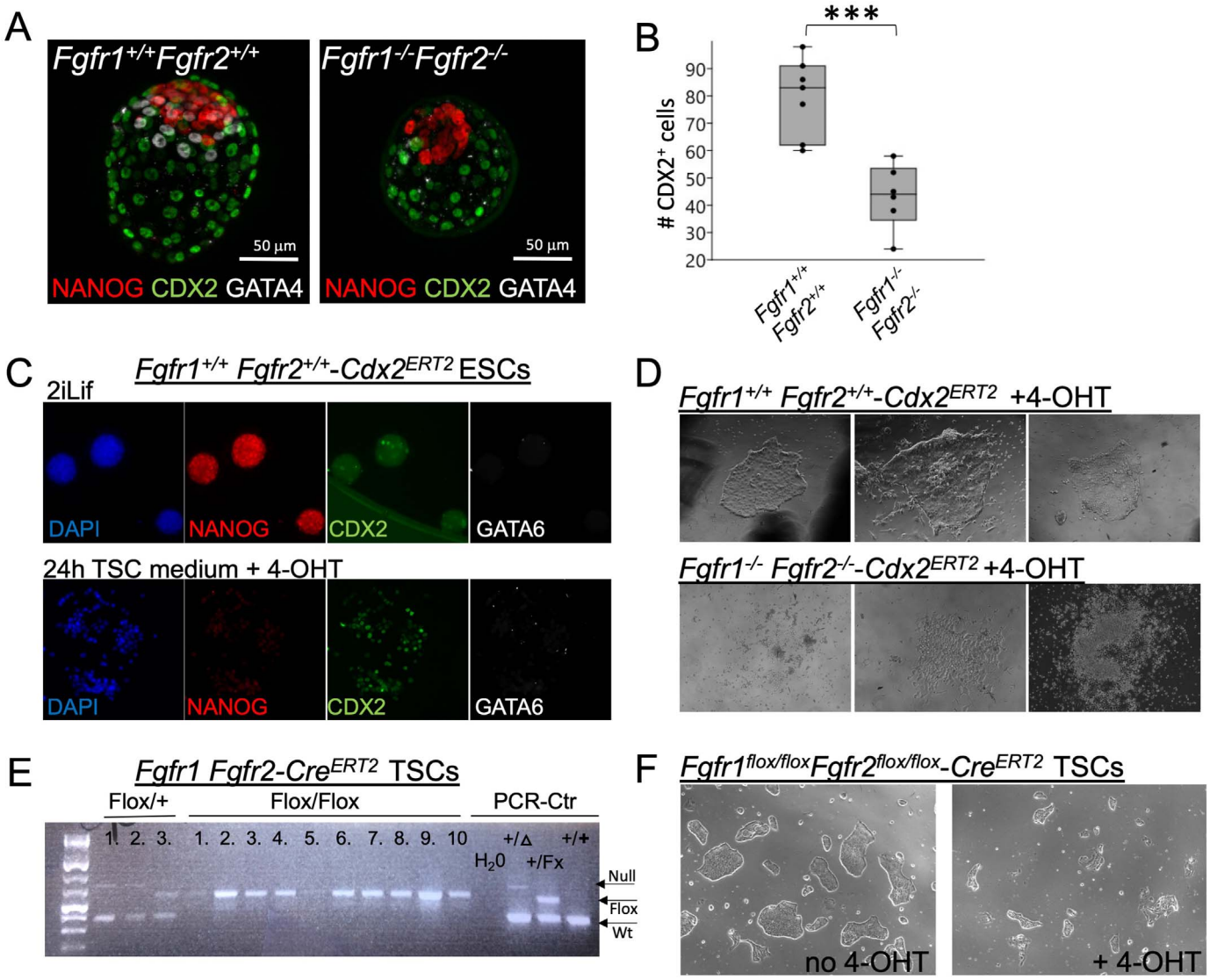

Fig. 6. *Fgfr1*$^{-/-}$ *Fgfr2*$^{-/-}$ embryos show reduced TE, and TSCs cannot be obtained. A and B, Optical section images of *Fgfr1*$^{-/-}$ *Fgfr2*$^{-/-}$ embryos isolated at E3.5 and cultured for 48 h show reduced numbers of CDX2 positive TE cells. Seven *Fgfr1*$^{+/+}$*Fgfr2*$^{+/+}$ and six *Fgfr1*$^{-/-}$*Fgfr2*$^{-/-}$ embryos were quantified, *** P < 0.001. C, Maximal projection images showing *Fgfr1*$^{+/+}$-*Cdx2*^{ERT2} puromycin resistant clones expressing CDX2 and downregulating NANOG upon 24 h of 4-OHT treatment. GATA6 is not expressed. D, brightfield images, showing three representative images for each genotype. Seven out of eight *Fgfr1*$^{+/+}$*Fgfr2*$^{+/+}$-*Cdx2*^{ERT2} ESC clones gave rise to TSC colonies, but none out of six *Fgfr1*$^{-/-}$*Fgfr2*$^{-/-}$-*Cdx2*^{ERT2} ESC clones gave rise to TSC colonies after two weeks in TSC medium with 1 µg/ml 4-OHT. E, PCR results of genomic DNA showing that two out of three *Fgfr1*$^{flox/+}$*Fgfr2*$^{flox/+}$-*Cre*^{ERT2} TSC clones exhibit CRE recombination after induction with 4-OHT. *Fgfr1*$^{flox/flox}$ *Fgfr2*$^{flox/flox}$-*Cre*^{ERT2} TSC colonies that escaped cell death did not undergo CRE recombination. F, Brightfield images showing 4-OHT treated *Fgfr1*$^{flox/flox}$ *Fgfr2*$^{flox/flox}$-*Cre*^{ERT2} cultures exhibiting cell death.

that maintained *Cdx2* expression in TE cells prevents *Fgfr1*$^{-/-}$ embryos from initiating the differentiation program required for implantation.

The polar TE forms the extra-embryonic ectoderm while maintaining a pool of proliferative TSCs (Tanaka et al., 1998). It lies in close proximity with the FGF4 producing EPI, whereas the mural TE, which lines the blastocoel cavity, undergoes differentiation into giant cells and initiates implantation. Further studies will be required to determine if FGFR1/2 indeed acts autonomously within the TE, or if the effects we observed are an indirect effect of a defect in EPI maturation or PrE development. FGF4 is also essential for maintaining TSCs proliferation and potency (Simmons and Cross, 2005; Tanaka et al., 1998). Upon removal of FGF4, TSCs differentiate into various TE lineages. We show that loss of either FGFR1 or FGFR2 does not impact the ability to establish or maintain TSCs. This may be due to the fact that both receptors are expressed in TSCs and the presence of one or the other receptor is sufficient for maintaining these cultures. Neither FGFR1 nor FGFR2 are required for the downregulation of TSC markers. However, *Fgfr1*$^{-/-}$ TSCs fail to upregulate TE differentiation markers upon FGF4 removal to the same extent as wild type cells. In contrast to the *in vivo* situation, *Fgfr1*$^{-/-}$ TSCs were able to downregulate *Cdx2*. However, we were unable to fully differentiate *Fgfr1*$^{-/-}$ TSCs into labyrinthine cells, spongiotrophoblast cells or trophoblast giant cells, the first TE lineage to be specified from proliferating TSCs *in vivo*. The elimination of both *Fgfr1* and *Fgfr2* led to a reduction in the number of TE cells in embryos, and we were unable to isolate double mutant TSCs, using two different approaches. Taken together, these results highlight a critical role for FGF signaling, in particular FGFR1, in TE development and TSC maintenance. Furthermore, they uncover an unsuspected requirement for FGFR1 signaling during trophoblast differentiation, which may be an important contributory factor in early pregnancy failure.

Acknowledgments

We thank Rob Krauss, Carla Mulas, Jenny Nichols and our laboratory colleagues for helpful discussions and for critical comments on the manuscript, and Austin Smith and Ken Jones for vectors. This

work was supported in part by the Tisch Cancer Institute at Mount Sinai (P30 CA196521 Cancer Center Support Grant) and by grants from NYSTEM (IIRP N11G-131) and NIH/NCI (RO1 DE022778) to P.S.

Appendix A. Supporting information

Supplementary data associated with this article can be found in the online version at doi:10.1016/j.ydbio.2018.12.008.

References

Betschinger, J., Nichols, J., Dietmann, S., Corrin, P.D., Paddison, P.J., Smith, A., 2013. Exit from pluripotency is gated by intracellular redistribution of the bHLH transcription factor Tfe3. Cell 153, 335–347.

Blij, S., Frum, T., Akyol, A., Fearon, E., Ralston, A., 2012. Maternal Cdx2 is dispensable for mouse development. Development 139, 3969–3972.

Brewer, J.R., Mazot, P., Soriano, P., 2016. Genetic insights into the mechanisms of Fgf signaling. Genes Dev. 30, 751–771.

Brewer, J.R., Molotkov, A., Mazot, P., Hoch, R.V., Soriano, P., 2015. Fgfr1 regulates development through the combinatorial use of signaling proteins. Genes Dev. 29, 1863–1874.

Chazaud, C., Yamanaka, Y., Pawson, T., Rossant, J., 2006. Early lineage segregation between epiblast and primitive endoderm in mouse blastocysts through the Grb2-MAPK pathway. Dev. Cell 10, 615–624.

Ciruna, B., Rossant, J., 2001. FGF signaling regulates mesoderm cell fate specification and morphogenetic movement at the primitive streak. Dev. Cell 1, 37–49.

Ciruna, B.G., Schwartz, L., Harpal, K., Yamaguchi, T.P., Rossant, J., 1997. Chimeric analysis of fibroblast growth factor receptor-1 (Fgfr1) function: a role for FGFR1 in morphogenetic movement through the primitive streak. Development 124, 2829–2841.

Cui, W., Taub, D.D., Gardner, K., 2007. qPrimerDepot: a primer database for quantitative real time PCR. Nucleic Acids Res 35, D805–D809.

Deng, C.X., Wynshaw-Boris, A., Shen, M.M., Daugherty, C., Ornitz, D.M., Leder, P., 1994. Murine FGFR-1 is required for early postimplantation growth and axial organization. Genes Dev. 8, 3045–3057.

Feldman, B., Poueymirou, W., Papaioannou, V.E., DeChiara, T.M., Goldfarb, M., 1995. Requirement of FGF-4 for postimplantation mouse development. Science 267, 246–249.

Fleming, T.P., Garrod, D.R., Elsmore, A.J., 1991. Desmosome biogenesis in the mouse preimplantation embryo. Development 112, 527–539.

Fleming, T.P., Johnson, M.H., 1988. From egg to epithelium. Annu. Rev. Cell Biol. 4, 459–485.

Funakoshi, S., Kong, J., Crissey, M.A., Dang, L., Dang, D., Lynch, J.P., 2010. Intestine-specific transcription factor Cdx2 induces E-cadherin function by enhancing the trafficking of E-cadherin to the cell membrane. Am. J. Physiol. Gastrointest. Liver Physiol. 299, G1054–G1067.

Gao, N., Kaestner, K.H., 2010. Cdx2 regulates endo-lysosomal function and epithelial cell polarity. Genes Dev. 24, 1295–1305.

Goldin, S.N., Papaioannou, V.E., 2003. Paracrine action of FGF4 during periimplantation development maintains trophectoderm and primitive endoderm. Genesis 36, 40–47.

Hammer, Ø., Harper, D.A.T., Ryan, P.D., 2001. PAST: Paleontological statistics software package for education and data analysis. Palaeontol. Electron. 4, 1–9.

Hatano, N., Mori, Y., Oh-hora, M., Kosugi, A., Fujikawa, T., Nakai, N., Niwa, H., Miyazaki, J., Hamaoka, T., Ogata, M., 2003. Essential role for ERK2 mitogen-activated protein kinase in placental development. Genes Cells 8, 847–856.

Hoch, R.V., Soriano, P., 2006. Context-specific requirements for Fgfr1 signaling through Frs2 and Frs3 during mouse development. Development 133, 663–673.

Jedrusik, A., Cox, A., Wicher, K.B., Glover, D.M., Zernicka-Goetz, M., 2015. Maternal-zygotic knockout reveals a critical role of Cdx2 in the morula to blastocyst transition. Dev. Biol. 398, 147–152.

Johnson, M.H., Ziomek, C.A., 1981. Induction of polarity in mouse 8-cell blastomeres: specificity, geometry and stability. J. Cell Biol. 91, 303–308.

Kang, M., Garg, V., Hadjantonakis, A.K., 2017. Lineage establishment and progression within the inner cell mass of the mouse blastocyst requires FGFR1 and FGFR2. Dev. Cell 41, 496–510.

Kang, M., Piliszek, A., Artus, J., Hadjantonakis, A.K., 2013. FGF4 is required for lineage restriction and salt-and-pepper distribution of primitive endoderm factors but not their initial expression in the mouse. Development 140, 267–279.

Kunath, T., Saba-El-Leil, M.K., Almousailleakh, M., Wray, J., Meloche, S., Smith, A., 2007. FGF stimulation of the Erk1/2 signalling cascade triggers transition of pluripotent embryonic stem cells from self-renewal to lineage commitment. Development 134, 2895–2902.

Molotkov, A., Mazot, P., Brewer, J.R., Cinalli, R.M., Soriano, P., 2017. Distinct requirements for Fgfr1 and Fgfr2 in primitive endoderm development and exit from pluripotency. Dev. Cell 41, 511–526.

Molotkov, A., Soriano, P., 2018. Distinct mechanisms for PDGF and FGF signaling in primitive endoderm development. Dev. Biol. 442, 155–161.

Mulas, C., Kalkan, T., Smith, A., 2017. NODAL secures pluripotency upon embryonic stem cell progression from the ground State. Stem Cell Rep. 9, 77–91.

Nichols, J., Silva, J., Roode, M., Smith, A., 2009. Suppression of Erk signalling promotes ground state pluripotency in the mouse embryo. Development 136, 3215–3222.

Niwa, H., Toyooka, Y., Shimosato, D., Strumpf, D., Takahashi, K., Yagi, R., Rossant, J., 2005. Interaction between Oct3/4 and Cdx2 determines trophectoderm differentiation. Cell 123, 917–929.

Ohinata, Y., Tsukiyama, T., 2014. Establishment of trophoblast stem cells under defined culture conditions in mice. PLoS One 9, e107308.

Ong, S.H., Guy, G.R., Hadari, Y.R., Laks, S., Gotoh, N., Schlessinger, J., Lax, I., 2000. FRS2 proteins recruit intracellular signaling pathways by binding to diverse targets on fibroblast growth factor and nerve growth factor receptors. Mol. Cell. Biol. 20, 979–989.

Saba-El-Leil, M.K., Vella, F.D., Vernay, B., Voisin, L., Chen, L., Labrecque, N., Ang, S.L., Meloche, S., 2003. An essential function of the mitogen-activated protein kinase Erk2 in mouse trophoblast development. EMBO Rep. 4, 964–968.

Simmons, D.G., Cross, J.C., 2005. Determinants of trophoblast lineage and cell subtype specification in the mouse placenta. Dev. Biol. 284, 12–24.

Stephenson, R.O., Rossant, J., Tam, P.P., 2012. Intercellular interactions, position, and polarity in establishing blastocyst cell lineages and embryonic axes. Cold Spring Harb. Perspect. Biol., 4, a008235.

Stephenson, R.O., Yamanaka, Y., Rossant, J., 2010. Disorganized epithelial polarity and excess trophectoderm cell fate in preimplantation embryos lacking E-cadherin. Development 137, 3383–3391.

Strumpf, D., Mao, C.A., Yamanaka, Y., Ralston, A., Chawengsaksophak, K., Beck, F., Rossant, J., 2005. Cdx2 is required for correct cell fate specification and differentiation of trophectoderm in the mouse blastocyst. Development 132, 2093–2102.

Sun, J., Stathopoulos, A., 2018. FGF controls epithelial-mesenchymal transitions during gastrulation by regulating cell division and apicobasal polarity. Development 145, dev161927. http://dx.doi.org/10.1242/dev.161927.

Sutherland, A., 2003. Mechanisms of implantation in the mouse: differentiation and functional importance of trophoblast giant cell behavior. Dev. Biol. 258, 241–251.

Tallquist, M.D., Soriano, P., 2000. Epiblast-restricted Cre expression in MORE mice: a tool to distinguish embryonic vs. extra-embryonic gene function. Genesis 26, 113–115.

Tanaka, S., Kunath, T., Hadjantonakis, A.K., Nagy, A., Rossant, J., 1998. Promotion of trophoblast stem cell proliferation by FGF4. Science 282, 2072–2075.

White, M.D., Zenker, J., Bissiere, S., Plachta, N., 2018. Instructions for assembling the early mammalian embryo. Dev. Cell 45, 667–679.

Xu, X., Weinstein, M., Li, C., Naski, M., Cohen, R.I., Ornitz, D.M., Leder, P., Deng, C., 1998. Fibroblast growth factor receptor 2 (FGFR2)-mediated reciprocal regulation loop between FGF8 and FGF10 is essential for limb induction. Development 125, 753–765.

Yamaguchi, T.P., Harpal, K., Henkemeyer, M., Rossant, J., 1994. fgfr-1 is required for embryonic growth and mesodermal patterning during mouse gastrulation. Genes Dev. 8, 3032–3044.

Yamanaka, Y., Lanner, F., Rossant, J., 2010. FGF signal-dependent segregation of primitive endoderm and epiblast in the mouse blastocyst. Development 137, 715–724.

Yu, K., Xu, J., Liu, Z., Sosic, D., Shao, J., Olson, E.N., Towler, D.A., Ornitz, D.M., 2003. Conditional inactivation of FGF receptor 2 reveals an essential role for FGF signaling in the regulation of osteoblast function and bone growth. Development 130, 3063–3074.